JOURNAL OF AGRICULTURAL AND FOOD CHEMISTRY

Analysis of Sugars in Chinese Rice Wine by Fourier Transform Near-Infrared Spectroscopy with Partial Least-Squares Regression

XIAOYING NIU,[†] FEI SHEN,[†] YANFEI YU,[‡] ZHANKE YAN,[†] KAI XU,[†] HAIYAN YU,[†] AND YIBIN YING*,[†]

College of Biosystems Engineering and Food Science, Zhejiang University, 268 Kaixuan Street, 310029 Hangzhou, and Shaoxing Testing Institute of Quality Technical Supervision, Shaoxing 312071, People's Republic of China

The feasibility of rapid analysis for oligosaccharides, including isomaltose, isomaltotriose, maltose, and panose, in Chinese rice wine by Fourier transform near-infrared (FT-NIR) spectroscopy together with partial least-squares regression (PLSR) was studied in this work. Forty samples of five brewing years (1996, 1998, 2001, 2003, and 2005) were analyzed by NIR transmission spectroscopy with seven optical path lengths (0.5, 1, 1.5, 2, 2.5, 3, and 5 mm) between 800 and 2500 nm. Calibration models were established by PLSR with full cross-validation and using high-performance anion-exchange chromatography coupled with pulsed amperometric detection as a reference method. The optimal models were obtained through wavelength selection, in which the correlation coefficients of calibration (r_{cal}) for the four sugars were 0.911, 0.938, 0.925, and 0.966, and the root-mean-square errors of calibrations were 0.157, 0.147, 0.358, and 0.355 g/L, respectively. The validation accuracy of the four models, with correlation coefficients of cross-validation (r_{cv}) being 0.718, 0.793, 0.681, and 0.873, were not very satisfactory. This might be due to the low concentrations of the four sugars in Chinese rice wine and the influence of some components having structures similar to those of the four sugars. The results obtained in this study indicated that the NIR spectroscopy technique offers screening capability for isomaltose, isomaltotriose, maltose, and panose in Chinese rice wine. Further studies with a larger Chinese rice wine sample should be done to improve the specificity, prediction accuracy, and robustness of the models.

KEYWORDS: Chinese rice wine; FT-NIR; oligosaccharide; HPAEC−PAD; PLSR

INTRODUCTION

Chinese rice wine is brewed from glutinous rice and wheat. Sugars in Chinese rice wine mainly come from hydrolysis reaction (catalyzed by an enzyme) of carbohydrates in glutinous rice and are one of the most important substances for the Chinese rice wine taste and smell (*1*). In the National Standard of China GB 13662-2000, Chinese rice wine is divided into four kinds according to the concentrations of the total sugars: dry type (total sugars ≤ 15 g/L); semidry type (15.1 g/L < total sugars < 40 g/L); semisweet type (40.1 g/L < total sugars <100 g/L); sweet type (total sugars > 100 g/L). In this study, the Chinese rice wine of the semidry type was investigated. Besides glucose and maltose, Chinese rice wine has several oligosaccharides such as isomaltose, isomaltotriose, and panose, which have been proved to be very valuable for human health (*2, 3*). The concentration of an individual sugar in Chinese rice wine provides much information on the general quality, flavor, and storage time, etc., and can be used to detect adulteration or fraud, to identify the variety, origin, and brewery, and even to optimize the brewing craft of Chinese rice wine. Hence, the determinations of individual sugars in Chinese rice wine are gaining more and more significance. Several works have been reported using the analytical technique of high-performance liquid chromatography (HPLC) for individual sugar analysis of Chinese rice wine (*4, 5*). The results obtained in these works can be used as references but are not universal due to the sample sizes adopted being too small (one or three samples).

There are some other chromatographic methods that can also be used to analyze individual sugars. High-performance anion-exchange chromatography coupled with pulsed amperometric detection (HPAEC−PAD) is one of the most useful techniques for oligosaccharide determination and has been employed to quantify specific concentrations of sugars in honey and wine samples (*6–9*). However, although chromatographic techniques have a high accuracy, some shortcomings, such as the complex sample preparation, high time consumption, and expensive cost

* To whom correspondence should be addressed. E-mail: ybying@zju.edu.cn. Phone/fax: 0086-571-86971885.
[†] Zhejiang University.
[‡] Shaoxing Testing Institute of Quality Technical Supervision.

10.1021/jf800993e CCC: $40.75
Published on Web 08/05/2008

Table 1. Elution Gradient Used in the HPAEC−PAD Method

time (min)	eluent A fraction (%)	eluent B fraction (%)	eluent C fraction (%)
0−11	84	16	0
20	81	16	3
40	78	16	6
40.1−50.1	20	80	0
50.2	84	16	0

of operation and maintenance, limit their application to rapid detection and process control.

Near-infrared (NIR) spectroscopy, which has advantages of being nondestructive, simple, fast, and without need of sample pretreatment (*10*), has been successfully applied to the determination of individual sugars in liquid samples such as fruit juice and honey on the basis of overtone and combination bands of specific functional groups (*11–17*). NIR spectroscopy utilizes the wavelength range from 780 to 2526 nm (ASTM) and provides much more complex structural information related to the vibration behaviors of combinations of bonds (*18*). Because of the complexity and high dimension of NIR spectral data, direct quantification analysis becomes impossible. Some chemometrics methods such as principal component regression (PCR) and partial least-squares (PLS) are needed to extract spectral features and investigate correlation between the spectra and component concentrations. In addition to the papers mentioned above, NIR together with these chemometrics methods has also been proved effective in detecting some other components in wine (*19–25*), culture broth (*26*), and wine vinegar and beer (*27–29*).

The aim of this study was to apply Fourier transform near-infrared (FT-NIR) spectroscopic techniques, with HPAEC−PAD as a reference method, for quantitative analysis of isomaltose, isomaltotriose, maltose, and panose in Chinese rice wine. The feasibility of using NIR spectroscopy to determine sugars of low concentration in Chinese rice wine samples was explored. The performance of PLS models using spectra of different optical path lengths and different spectral regions was evaluated. The sensitive wavelengths of the four sugars in NIR spectra were also investigated on the basis of partial least-squares regression (PLSR) loading spectra.

MATERIALS AND METHODS

Samples. Forty Chinese rice wine samples obtained from the Pagoda brand Shaoxing wine brewery (Zhejiang Cereal, Oils, and Foodstuffs Import and Export Co., Ltd., Shaoxing, Zhejiang Province, China), including eight of 1 year age, 3 year age, 5 year age, 8 year age, and 10 year age, were used in this study. All these samples were directly taken from the storage containers and without any additive.

Reagents. Analytical grade isomaltose, D-(+)-maltose monohydrate, D-panose, and isomaltotriose were purchased from Sigma-Aldrich (Sigma, St. Louis, MO). Standard stock solutions were prepared from 1 g of the appropriate sugar dissolved in 100 mL of Milli-Q distilled water. Aqueous solutions of sodium hydroxide and sodium acetate were purchased from Dionex Corp.

Spectral Measurements. Samples taken from freshly opened bottles of Chinese rice wine were scanned in transmission mode (800−2500 nm) using a scanning spectrometer, Nexus FT-NIR (Thermo Nicolet Corp., Madison, WI), with an interferometer, an InGaAs detector, and a broad-band light source (quartz tungsten halogen, 50 W). NIR spectral data were collected using OMNIC software (Thermo Nicolet Corp.) and stored in absorbance format. Samples were scanned in demountable liquid cells of different optical path lengths (0.5, 1, 1.5, 2, 2.5, 3, and 5 mm; Pike Technologies, Madison, WI) with air as the reference at room temperature. All samples were shaken before scanning. The mirror velocity was 0.9494 cm s^{-1}, and the resolution was 2 cm^{-1}. The spectrum of each sample was the average of 32 successive scans. The spectral regions with an absorbance value equal to or higher than 1.5 were not used in spectral analysis due to the zero transmissivity and the fact that they are considered saturated.

Anion-Exchange Chromatography. Prior to the FT-NIR measurement, HPAEC−PAD was applied to quantitative determination of sugars in Chinese rice wine, and the results were used as reference data in FT-NIR analysis. All samples were analyzed by a Dionex Instrument (Dionex Corp.) consisting of a pulsed amperometric detector (model ED 50) with a gold electrode as the working electrode and a pH Ag|AgCl combination reference electrode (set to the AgCl mode), a gradient pump (model GP 50), a Dionex CarboPac PA10 column (2 × 250 mm) suited for mono-, di-, tri-, and oligosaccharide analysis, and a guard column (2 × 50 mm). A three-step PAD setting was used with the following potentials and durations: $E_1 = +0.05$ V ($t_1 = 400$ ms); $E_2 = +0.75$ V ($t_2 = 200$ ms); $E_3 = -0.15$ V ($t_3 = 400$ ms). Analyses were performed using Milli-Q distilled water as eluent A, sodium hydroxide (250 mmol/L) as eluent B, and sodium acetate (1.0 mmol/L) as eluent C. The elution gradient is shown in **Table 1**. The flow rate was fixed at 0.25 mL/min, and the column temperature was kept at 30 °C. A 10 mL aliquot of Chinese rice wine was diluted 500 times, passed through a 0.22 μm porosity filter, and then injected manually. The injection volume was 20 μL. All experiments were conducted at room temperature. The chromatogram acquisition was performed with the PeakNet 6.0 software suite.

Chemometrics and Data Analysis. Chemometrics analysis were performed using a commercial software package, TQ Analyst (Thermo Electron Corp., Madison, WI). Stepwise multiple linear regressions (SMLRs) were used, but the results were worse than those obtained using PLSR. Therefore, PLSR was adopted in this study. Spectra were exported from OMNIC software in absorbance format to TQ Analyst software before analysis.

Wavelength Selection. NIR spectra typically consist of broad, weak, nonspecific, extensively overlapped bands and may have hundreds or thousands of wavelength variables (*30*). Some of these variables may contain useless or irrelevant information for the calibration model such as noise and background, which can worsen the predictive ability of the whole model (*31*). In wavelength selection, one or several subsets of spectral regions, with which the established calibration model presents better performance and gives minimum errors in validation, were selected. Wavelength selection not only enhances the stability of the model resulting from the collinearity in multivariate spectra but also helps in interpreting the relationship between the model and the sample compositions (*11*). In this study, the full spectra were divided into four regions, 800−1250, 1250−1650, 1650−2200, and 2200−2500 nm, according to the main absorption bands. Calibration models were established on each spectral region, the combination bands of 1250−1650 and 1650−2200 nm, and the full spectra.

PLSR. All spectral data were pretreated using the mean centering technique. The Student residual and leverage were employed to detect outliers. PLSR and leave-one-out cross-validation were used to develop calibration models to investigate which optical path length of the seven was best for predicting the concentrations of sugars in the samples of Chinese rice wine. The most effective spectral group was used in further analysis. PLSR is a multivariate statistical method that can be used to relate two independent data matrices. In PLSR, the original spectral variables are projected onto a small number of new latent variables (LVs, also called factors). The first several factors usually account for the greatest amount of spectral variance. The individual factors calculated from the PLS spectral decomposition are useful for finding spectral regions of importance in the calibration of certain components (*32*). Here PLS models with 1−20 factors were investigated, and the optimum number of factors used in PLSR was determined by the lowest value of the predicted residual error sum of squares (PRESS).

The PLS models were validated by leave-one-out cross-validation called full cross-validation. Samples in the calibration set were divided into two sets, and the dependent variables of one set could be predicted from the calibration models of the remaining samples. The process was repeated until each sample in the calibration set had been predicted once. Cross-validation of a calibration model makes it possible to select the optimum number of latent variables or factors, that is, the number giving the minimum prediction error for the calibration set (*33*). The

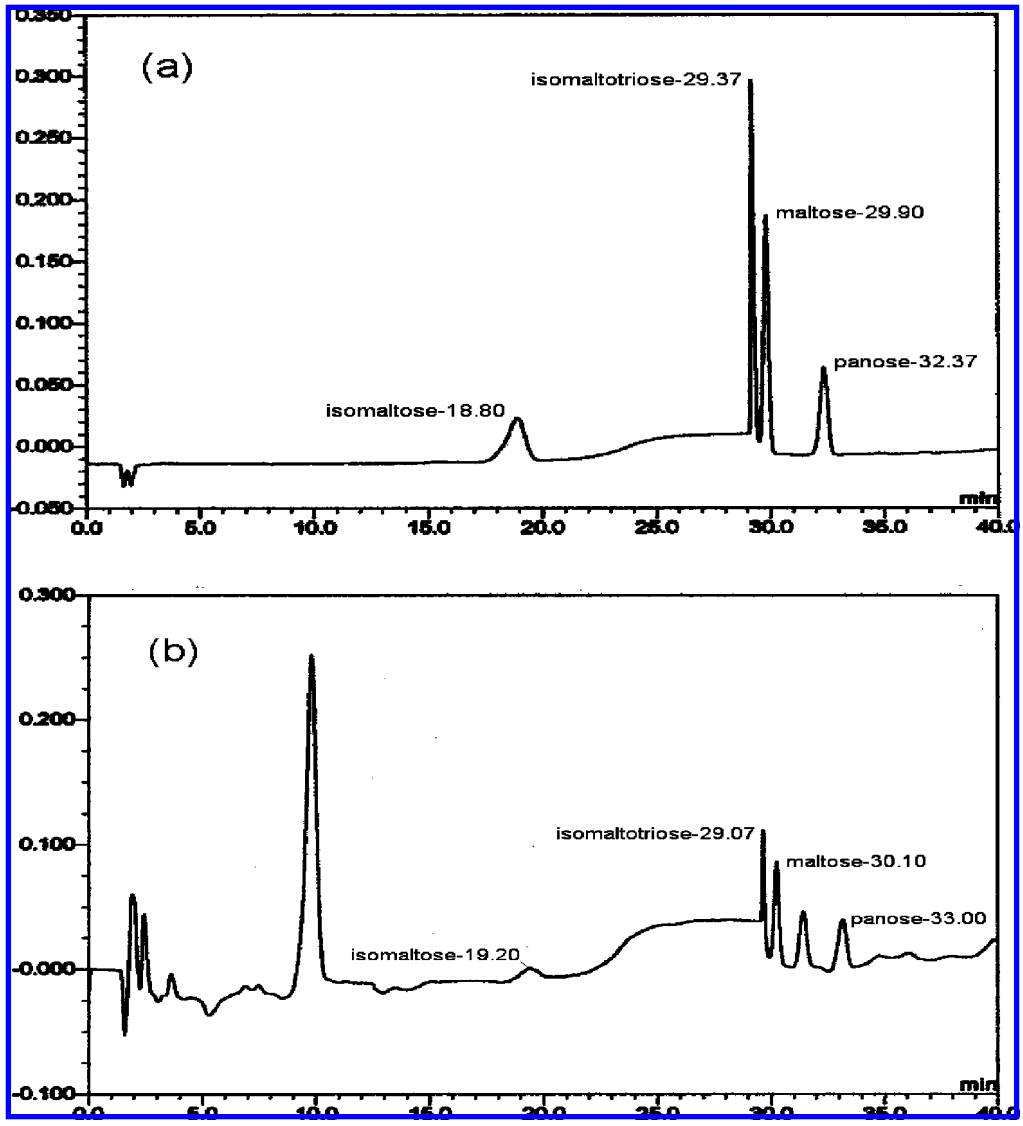

Figure 1. (**a**) Separation of an isomaltose, isomaltotriose, maltose, and panose standard and (**b**) separation of a Chinese rice wine sample.

Table 2. Summary of Isomaltose, Isomaltotriose, Maltose, and Panose Values in Chinese Rice Wine Determined by AEC

property	number of samples	range	mean	standard deviation
isomaltose concn (g/L)	40	0.666−2.190	1.271	0.383
isomaltotriose concn (g/L)	40	1.266−3.005	1.992	0.439
maltose concn (g/L)	40	0.298−3.671	1.403	0.992
panose concn (g/L)	40	1.269−5.708	3.461	1.396

performance of the calibration models is assessed from the value of the root-mean-square error of cross-validation (RMSECV) and the value of the residual predictive deviation (RPD), which were defined as follows:

$$\mathrm{RMSECV} = \sqrt{\frac{\sum_{i=1}^{I} (y_i - \hat{y}_i)^2}{I}}, \quad \mathrm{RPD} = \frac{\mathrm{S.D.}}{\mathrm{RMSECV}}$$

where y_i and $\hat{y}_i$ are the amounts of measured sugars and predicted sugars, respectively, for all predicted samples i (1, 2, . . . , i) and S.D. is the standard deviation for the calibration samples. In addition, the correlation coefficient (r) between the amounts of the measured sugars and the predicted sugars and the root-mean-square error of calibration (RMSEC) were included in the calibration statistics. Referring to the criteria used by other researchers (*24*), the calibration models with r values (in calibration) higher than 0.94 as well as RMSECV values higher than RMSEC and lower than 2(RMSEC) are considered to have excellent precision. R values between 0.84 and 0.94 indicate good precision, as well as RMSECV values in the range of RMSEC−2(RMSEC). For r values lower than 0.84, the calibration model can only be used for screening purposes, distinguishing only among low, medium, and high values, and for r values lower than

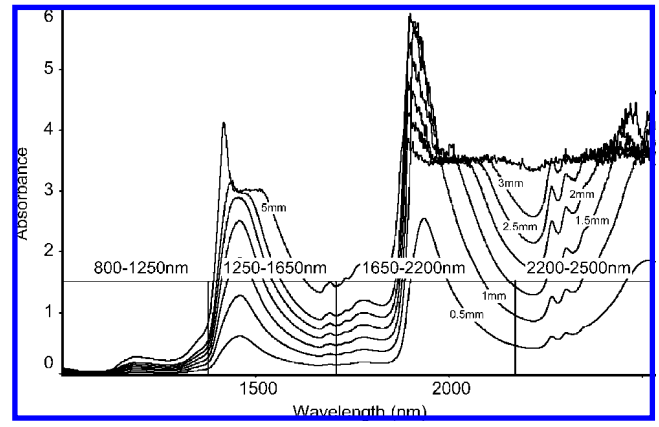

Figure 2. Average NIR absorbance spectra of 40 Chinese rice wine samples for 7 different optical path lengths (0.5, 1, 1.5, 2, 2.5, 3, and 5 mm).

Table 3. Spectral Regions Actually Used To Establish PLS Models of Different Optical Path Lengths

optical path length (mm)	spectral regions for the calibration model (nm)
0.5	800−1250, 1250−1650, 1650−1900 and 2000−2200, 2200−2450
1	800−1250, 1250−1650, 1650−1880 and 2090−2200, 2200−2340
1.5	800−1250, 1250−1425 and 1500−1650, 1650−1876 and 2156−2200, 2200−2250
2	800−1250, 1250−1409 and 1520−1650, 1650−1868
2.5	800−1250, 1250−1400 and 1545−1650, 1650−1864
3	800−1250, 1250−1397 and 1569−1650, 1650−1856
5	800−1250, 1250−1389 and 1630−1650, 1650−1725

Table 4. Best Calibration Models of Different Optical Path Lengths for Sugars in Chinese Rice Wine Samples Based Only on the Full Spectra

		calibration		cross-validation			
compd	optical path length (mm)	r_{cal}	RMSEC	r_{cv}	RMSECV	RPD	no. of factors
isomaltose	2.5	0.822	0.217	0.746	0.255	1.50	4
isomaltotriose	5	0.938	0.147	0.793	0.259	1.69	5
maltose	0.5	0.962	0.257	0.754	0.625	1.59	8
panose	0.5	0.912	0.559	0.836	0.755	1.85	6

Table 5. Summary of Optimal Calibration Models for Sugars in Chinese Rice Wine Samples Using the Selected Spectral Region

			calibration		cross-validation			
compd	optical path length (mm)	spectral region (nm)	r_{cal}	RMSEC	r_{cv}	RMSECV	RPD	no. of factors
isomaltose	3	1250–1650	0.911	0.157	0.718	0.267	1.43	5
isomaltotriose	5	800–2500	0.938	0.147	0.793	0.259	1.69	5
maltose	1	2200–2500	0.925	0.358	0.681	0.7	1.42	4
panose	1	2200–2500	0.966	0.355	0.873	0.667	2.09	4

0.70, the model can only determine high and low values. Anyhow, the calibration models with the highest r (in both calibration and cross-validation) as well as the lowest RMSEC and RMSECV with the least difference from each other were considered optimal. The RPD value is an index used to check the robustness of a model, and relatively high RPD values indicate models having greater power to predict the chemical composition (*23*). A cutoff point of 3 was recommended by researchers, and a higher RPD value would be considered very good for prediction purposes (*34*).

RESULTS AND DISCUSSION

Anion-Exchange Chromatography Analysis. In this analysis, each sample was measured in duplicate to check the reproducibility of the anion-exchange chromatography measurements. **Figure 1a** shows the separation of an isomaltose, isomaltotriose, maltose, and panose standard mixture with an analytical time of <40 min. The concentrations of isomaltose, isomaltotriose, maltose, and panose are 5.3, 10.1, 11.5, and 7.3 mg/L, respectively. **Figure 1b** shows the separation of a Chinese rice wine sample. The retention times of the four sugars in the chromatographic profile are consistent with the retention times in the standard mixture (**Figure 1**). Besides the peaks of the four sugars, there are several other peaks in **Figure 1b**, which indicate that some other nonidentified compounds in Chinese rice wine can also be detected under this condition. The sum-

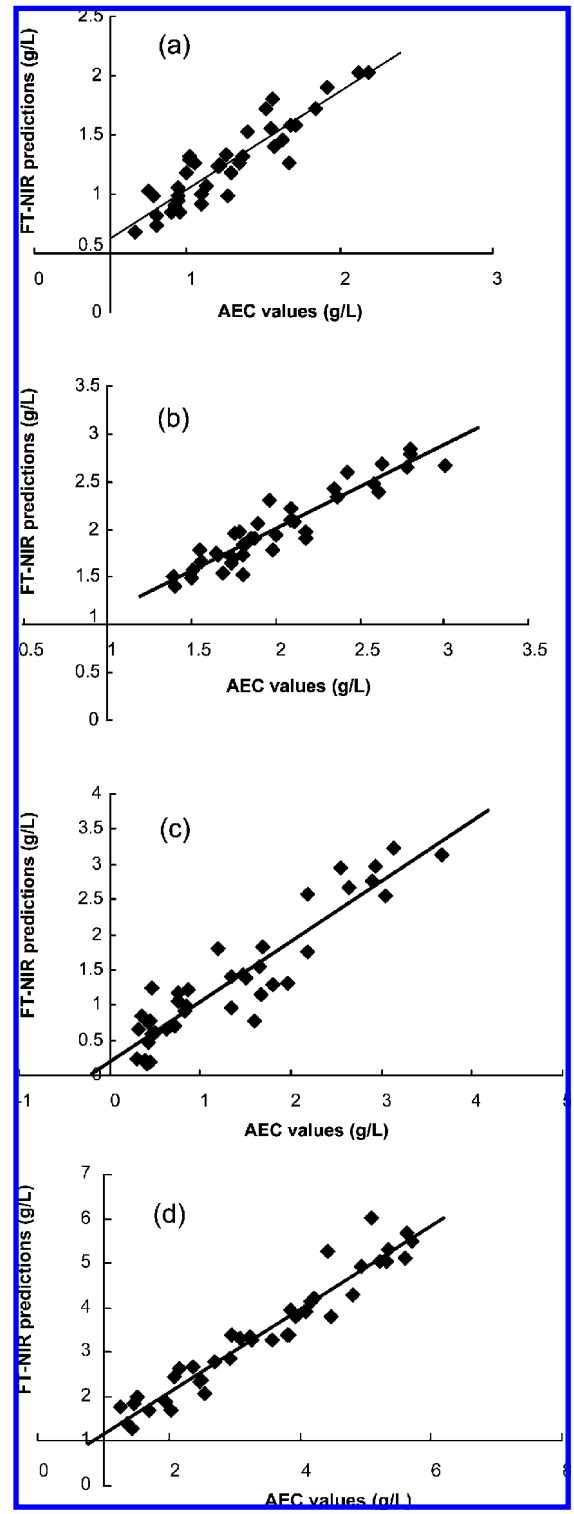

Figure 3. Correlation statistics between AEC values and FT-NIR predictions: (**a**) isomaltose (optical path length of 3 mm, 1250−1650 nm); (**b**) isomaltotriose (optical path length of 5 mm, 800−2500 nm); (**c**) maltose (optical path length of 1 mm, 2200−2500 nm); (**d**) panose (optical path length of 1 mm, 2200−2500 nm).

mary of AEC results is shown in **Table 2**. It can be seen that the range of sugar values in Chinese rice wine encompasses (isomaltotriose, maltose, and panose) or is close to (isomaltose) the values of similar sugars reported by previous researchers (*4, 35*). The tiny difference might be due to the different sample source or aging time. The variation ranges and standard deviations of all four sugars determined in this study were generally greater

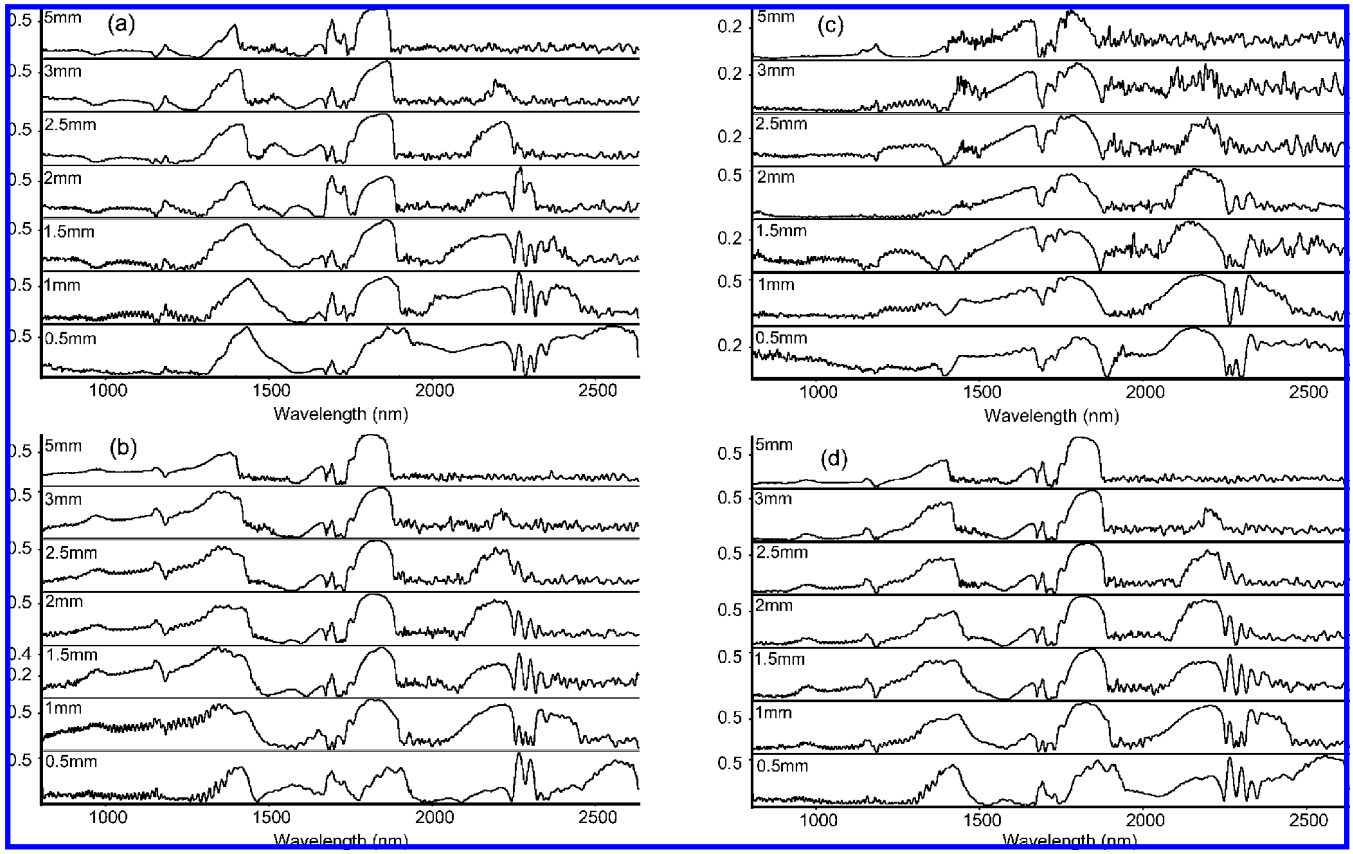

Figure 4. Regression coefficient of the calibration models with different optical path lengths in Chinese rice wine samples based on the full spectra: (**a**) isomaltose; (**b**) isomaltotriose; (**c**) maltose; (**d**) panose.

than those reported previously (*4*), possibly representing a large distinction in the aging time of the samples used in this study (1, 3, 5, 8, and 10 years).

Spectral Features. Figure 2 shows the average NIR absorbance spectra of 40 Chinese rice wine samples for 7 different optical path lengths (from bottom to top, respectively, 0.5, 1, 1.5, 2, 2.5, 3, and 5 mm). Just as in the literature previously published (*12, 20*), the absorbance in the full spectral bands becomes more intense with increasing optical path length, which causes more spectral regions to become saturated and subsequently reduces the wavelength range that can be used in spectral analysis. After removal of the saturated bands (absorbance value above 1.5), the spectral regions actually used to establish PLS models of different optical path lengths are shown in **Table 3**.

At the same time, it can be seen in **Figure 2** that the spectra of Chinese rice wine samples show intense absorption bands at 1450 nm related to the first O−H overtone in water or carbohydrate and at 1900−1950 nm related to the combination of stretching and deformation of the O−H group in water (*36, 37*). The small absorption band at 1690 nm might be related to the $-CH_3$ stretch first overtone or C−H groups in aromatic compounds, that at 1790 nm to O−H bonds associated with sucrose, fructose, and glucose in fruit juices (*17, 38*), that at 2266 nm likely to C−H combination bands of methanol, and that at 2302 nm to the combination band of C−H stretching and deformation of C−H from the $-CH_2$ group (*21, 39, 40*). The smaller absorption bands at 990 and 1185 nm are reported to be due to the second overtone of the O−H stretching band and the combination of the first overtone of the O−H stretching and the O−H bending bands from water, respectively (*41*).

Selection of the Optimum PLS Models. Student residual and leverage values of 40 Chinese rice wine samples were calculated, and one sample considered abnormal was removed as an outlier from the isomaltose, isomaltotriose, maltose, and panose values. The remaining 39 samples were used to establish PLS calibration models. **Table 4** shows the best calibration models for isomaltose, isomaltotriose, maltose, and panose in Chinese rice wine samples on the full spectra (without variable selection). The best calibration results of the full spectra were selected from models of different optical path lengths and obtained with an optical path length of 2.5 mm for isomaltose, 5 mm for isomaltotriose, and 0.5 mm for maltose and panose. The correlation coefficients of isomaltose calibration were lower than 0.84 and higher than 0.70, so this model could only determine low, medium, and high values. The calibrations of isomaltotriose and panose had good precision, but the values of RMSEC and RMSECV in the panose calibrations were high and need to decrease. The calibrations for maltose gave marked differences between RMSEC and RMSECV (RMSECV > 2(RMSEC)) and show a need to improve the robustness of the models. All four RPD values were lower than 3, which indicated that the validation quality of all four models should be improved.

Five fragments of the full spectra selected in the above paragraph, including 800−1250, 1250−1650, 1650−2200, 2200−2500, and 1250−2200 nm, were used to establish calibration models. The optimal calibration model was obtained with an optical path length of 3 mm and a spectral region of 1250−1650 nm for isomaltose, 5 mm and 800−2500 nm (actually 800−1725 nm; refer to **Table 3**) for isomaltotriose, and 1 mm and 2200−2500 nm for maltose and panose (**Table 5**). Calibration results based on selected spectral regions presented better performance than those based on the full spectra. The calibration models for isomaltose, isomaltotriose, and maltose had good precision, and for panose an excellent precision was obtained. Compared with those for the full spectra, the RPD value for panose gains an increase, while those for

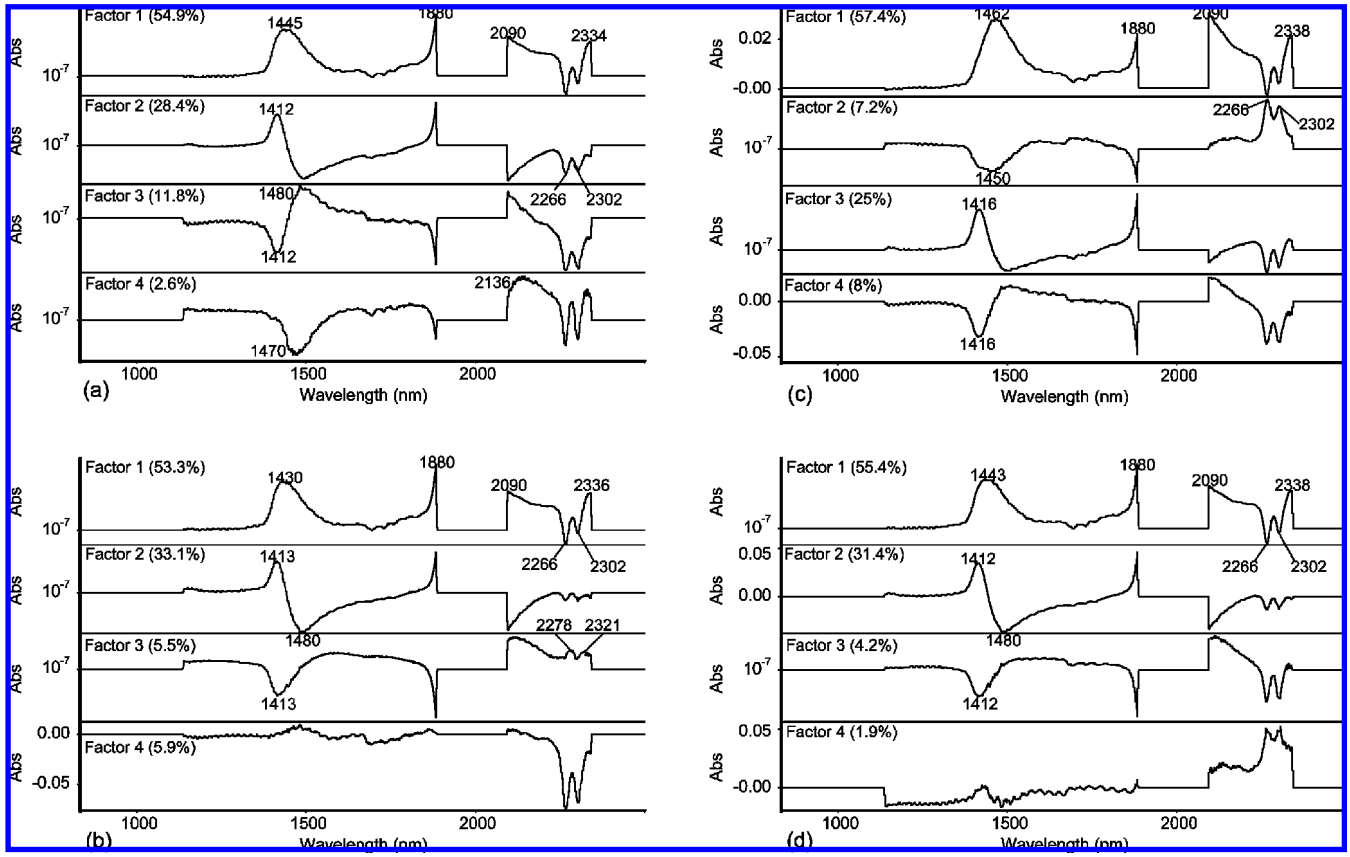

Figure 5. Loading spectra of the first four factors for (**a**) isomaltose, (**b**) isomaltotriose, (**c**) maltose, and (**d**) panose.

isomaltose and maltose decrease slightly. Because of the small size of the Chinese rice wine sample in this study, all 40 samples were used in the calibration and the validation quality of the calibration models was evaluated by r_{cv} and RMSECV of cross-validation as well as RPD. It could be observed that the validation qualities of the four optimal models with a low value of the index r_{cv} (0.718, 0.793, 0.618, and 0.873 for isomaltose, isomaltotriose, maltose, and panose, respectively) were all not very satisfactory and need improvement, as does the index RPD (**Table 5**). Although the low RPD values (1.42−2.09) indicated that the validation qualities of the models need improvement, the four models could be used for screening purposes because the other indexes in the calibrations were good. The AEC-measured values versus FT-NIR-predicted values from the optimal calibration model for the four sugars are shown in **Figure 3**.

Because of the low concentrations of isomaltose, isomaltotriose, maltose, and panose as well as the influence of other complicated components in Chinese rice wine, the PLS models for the four sugars, especially isomaltose and maltose, show a poor validation accuracy. However, the results obtained in this study show the potential of NIR with the reference method of HPAEC−PAD to determine isomaltose, isomaltotriose, maltose, and panose in Chinese rice wine rapidly and economically. Because the small sample size might not fully represent the features of Chinese rice wine, further studies should be done to improve the specificity, prediction accuracy, and robustness of the models.

To investigate the correlation between the spectra and sugar concentrations, regression coefficient plots of different optical path lengths based on the full spectra were analyzed. Curves of regression coefficients for different optical path lengths for isomaltose had very similar shapes, which also happened for isomaltotriose, maltose, and panose (**Figure 4**). Referring to **Figure 4** and **Table 3**, the calibrations for isomaltose all have high regression coefficients around 1430 nm and maxima around 1850 nm, for isomaltotriose, the regression coefficients show high values around 1350 nm and maxima around 1820 nm, and for maltose the maxima appear around 1660 and 1770 nm and for panose around 1415 and 1820 nm. Regarding the curves for 0.5, 1, and 1.5 mm optical path lengths, high correlations are also obtained in the range 2200−2500 nm.

For the four sugars, the performances of the models for different optical path lengths were contrasted, and differences for neither the full spectra nor the selected spectral regions were obvious. At the same time, the optimal models for the four sugars after wavelength selection were not the same in optical path lengths, with the best ones based on the full spectra. This illustrates that, in this study, although optical path lengths have a small effect on the calibration, the combination of different optical path lengths and wavelength selection can be effective to improve the performance of the calibration models.

Factor Loading Analysis. PLSR loading spectra based on the full spectra were investigated to extract absorption features of isomaltose, isomaltotriose, maltose, and panose in Chinese rice wine samples. To avoid excessively weak and intense absorbance due to short and long optical path lengths, the spectra for the 1 mm path length were selected for analysis. The spectral ranges of 1880−2090 and 2340−2500 nm in **Figure 5** were removed from the analysis because of saturation.

Figure 5 shows the loading spectra of the first four factors for isomaltose (**a**), isomaltotriose (**b**), maltose (**c**), and panose (**d**). The first four factors account for 97.7% (isomaltose), 97.8% (isomaltotriose), 97.6% (maltose), and 92.9% (panose) of the variation in the spectra, with factor 1 explaining more than half of the variation, being, respectively, 54.9%, 53.3%, 57.4%, and 55.4%.

For isomaltose (**Figure 5a**), the highest loadings of factors 1 and 2 were both at 1880 nm, the edge of the saturated region, which might be related to O−H stretching, as were those for isomaltotriose and panose. Factor 3 has the highest loadings at 1480 nm related to the first O−H stretch in glucose. The highest loadings of factor 4 at 2136 nm are reported to be related to the combination of N−H stretching and C═O stretching in amino acids (*42*). The peaks at 1445 and 1412 nm of factors 1 and 2, and the inverse peaks at 1410 and 1470 nm of factors 3 and 4, were all around the absorption wavelength of 1450 nm in the original spectra and might be related to the first O−H overtone in water or carbohydrate just as mentioned above. Factor 1 also has a peak at 2334 nm likely related to the combination of C−H stretching and deformation (*36*).

In **Figure 5b**, factor 3 for isomaltotriose has peaks at 2278 reported to be related to absorption of sucrose (*14*) and 2321 nm related to the combination of C−H stretching and deformation (*36*). Loading spectra of the first four factors for the four sugars all have peaks at 2266 and 2302 nm, inverse or not, which indicated that the two wavelengths might be related to some groups simultaneously contained in the four sugars and the two wavelengths might be appropriate for estimation of the total content of the four sugars.

Combined with the results from regression coefficients, some wavelengths, such as those around 1450, 1880, and 2090 nm as well as around 2300 nm, were sensitive for isomaltose, isomaltotriose, maltose, and panose analysis. The sensitive wavelengths obtained from loading spectral analysis were summarized as follows: 1412, 1445, 1480, 1880, 2090, 2334, 2266, and 2302 nm for isomaltose, 1413, 1430, 1480, 1880, 2090, 2336, 2266, 2302, 2278, and 2321 nm for isomaltotriose, 1416, 1450, 1462, 1880, 2090, 2338, 2266, and 2302 nm for maltose, and 1412, 1443, 1480, 1880, 2090, 2338, 2266, and 2302 nm for panose. It is well-known that the four sugars all have C−H and O−H groups as the main absorbance in NIR spectra, and the similarity in structure can lead to a serious overlap in absorption wavelength. The investigation of wavelength sensitivity would be very useful in the Chinese rice wine industry and provides the possibility to develop a simple and rapid device. This is just a preliminary result, and further investigation should be done to prove the sensitivity of these wavelengths for specific sugars.

ACKNOWLEDGMENT

We thank the Pagoda brand Shaoxing rice wine brewery for providing the samples.

LITERATURE CITED

(1) Wang, J. G.; Xu, L. Features of millet wine and its prospects. *Jiangsu Condiment Subsidiary Food.* **2005**, *22* (6), 5–9.

(2) Fan, H. D.; Qiao, D. L. Study for nutritional value of rice wine. *J. Northwest Minorities Univ. (Nat. Sci.)* **2000**, *21* (2), 47–49.

(3) Que, F.; Mao, L. C.; Zhu, C. G.; Xie, G. F. Antioxidant properties of Chinese yellow wine, its concentrate and volatiles. *Lebensm.-Wiss. Technol.* **2006**, *39*, 111–117.

(4) Xie, G. F.; Dai, J.; Zhao, G. A.; Chen, S. W.; Shuai, G. L. Functional oligosaccharides in rice wine and its health function. *China Brew.* **2005**, No. 2, 39−40.

(5) Chen, Y.; Fan, K. Q.; Tang, Q. L. Determination of sugars, alcohols and acids in fermented liquors by liquid chromatography. *Liquor Making* **2006**, *33* (1), 73–74.

(6) Cataldi, T. R. I.; Nardiello, D. Determination of free proline and monosaccharides in wine samples by high-performance anion-exchange chromatography with pulsed amperometric detection (HPAEC-PAD). *J. Agric. Food Chem.* **2003**, *51*, 3737–3742.

(7) Morales, V.; Corzo, N.; Sanz, M. L. HPAEC-PAD oligosaccharide analysis to detect adulterations of honey with sugar syrups. *Food Chem.* **2008**, *107*, 922–928.

(8) Pastore, P.; Lavagnini, I.; Versini, G. Ion chromatographic determination of monosaccharides from trace amounts of glycoside isolated from grape musts. *J. Chromatogr.* **1993**, *634*, 47–56.

(9) Bernal, J. L.; Del Nozal, M. J.; Toribio, L.; Del Alamo, M. HPLC analysis of carbohydrates in wine and instant coffees using anion exchange chromatography coupled to pulsed amperometric detection. *J. Agric. Food Chem.* **1996**, *44*, 507–511.

(10) Chen, J.; Arnold, M. A.; Small, G. W. Comparison of combination and first overtone spectral regions for near-infrared calibration models for glucose and other biomolecules in aqueous solutions. *Anal. Chem.* **2004**, *76*, 5405–5413.

(11) Liu, Y. D.; Ying, Y. B.; Yu, H. Y.; Fu, X. P. Comparison of the HPLC method and FT-NIR analysis for quantification of glucose, fructose, and sucrose in intact apple fruits. *J. Agric. Food Chem.* **2006**, *54*, 2810–2815.

(12) Rambla, F. J.; Garrigues, S.; de la Guardia, M. PLS-NIR determination of total sugar, glucose, fructose and sucrose in aqueous solutions of fruit juices. *Anal. Chim. Acta* **1997**, *344*, 41–53.

(13) Qiu, P. Y.; Ding, H. B.; Tang, Y. K.; Xu, R. J. Determination of chemical composition of commercial honey by near-infrared spectroscopy. *J. Agric. Food Chem.* **1999**, *47*, 2760–2765.

(14) Rodriguez-Saona, L. E.; Fry, F. S.; McLaughlin, M. A.; Calvey, E. M. Rapid analysis of sugars in fruit juices by FT-NIR spectroscopy. *Carbohydr. Res.* **2001**, *336*, 63–74.

(15) Kawano, S.; Sato, T.; Iwamoto, M. Determination of sugars in Satsuma orange using NIR transmittance. In *Proceedings of the Fourth International Conference on NIR Spectroscopy*; Murray, I., Ed.; School of Agriculture: Aberdeen, U.K., 1992.

(16) Lanza, E.; Li, B. W. Application for near infrared spectroscopy for predicting the sugar contents of fruit juices. *J. Food Sci.* **1984**, *49*, 995–998.

(17) Giangiacomo, R.; Dull, G. G. Near infrared spectrophotometric determination of individual sugars in aqueous mixtures. *J. Food Sci.* **1986**, *51*, 679–683.

(18) Reid, L. M.; O'Donnell, C. P.; Downey, G. Recent technological advances for the determination of food authenticity. *Trends Food Sci. Technol.* **2006**, *17*, 344–353.

(19) Yu, H. Y.; Ying, Y. B.; Fu, X. P.; Lu, H. S. Quality determination of Chinese rice wine based on fourier transform near infrared spectroscopy. *J. Near Infrared Spectrosc.* **2006**, *14* (1), 37–44.

(20) Yu, H. Y.; Xu, H. R.; Ying, Y. B.; Xie, L. J.; Zhou, Y.; Fu, X. P. Prediction of trace metals in chinese rice wine by Fourier transform near-infrared spectroscopy. *Trans. ASABE* **2006**, *49* (5), 1463–1467.

(21) Dambergs, R. G.; Kambouris, A.; Francis, I. L.; Gishen, M. Rapid analysis of methanol in grape-derived distillation products using near-infrared transmission spectroscopy. *J. Agric. Food Chem.* **2002**, *50*, 3079–3084.

(22) Sauvage, L.; Frank, D.; Stearne, J.; Millikan, M. B. Trace metal studies of selected white wines: an alternative approach. *Anal. Chim. Acta* **2002**, *458*, 223–230.

(23) Cozzolino, D.; Kwiatkowski, M. J.; Parker, M.; Cynkar, W. U.; Dambergs, R. G.; Gishen, M.; Herderich, M. J. Prediction of phenolic compounds in red wine fermentations by visible and near infrared spectroscopy. *Anal. Chim. Acta* **2004**, *513*, 73–80.

(24) Urbano-Cuadrado, M.; Luque de Castro, M. D.; Perez-Juan, P. M.; Garcia-Olmo, J.; Gomez-Nieto, M. A. Near infrared reflectance spectroscopy and multivariate analysis in enology. Determination or screening of fifteen parameters in different types of wines. *Anal. Chim. Acta* **2004**, *527*, 81–88.

(25) Urbano-Cuadrado, M.; Luque de Castro, M. D.; Perez-Juan, P. M.; Gomez-Nieto, M. A. Comparison and joint use of near infrared spectroscopy and Fourier transform mid infrared spectroscopy for the determination of wine parameters. *Talanta* **2005**, *66*, 218–224.

(26) Yano, T.; Aimi, T.; Nakano, Y.; Tamaf, M. Prediction of the concentrations of ethanol and acetic acid in the culture broth of

a rice vinegar fermentation using near-infrared spectroscopy. *J. Ferment. Bioeng.* **1997**, *5* (84), 461–465.
(27) Saiz-Abajo, M. J.; Gonzalez-Saiz, J. M.; Pizarro, C. Prediction of organic acids and other quality parameters of wine vinegar by near-infrared spectroscopy: a feasibility study. *Food Chem.* **2006**, *99*, 615–621.
(28) Inon, F. A.; Garrigues, S.; de la Guardia, M. Combination of mid- and near-infrared spectroscopy for the determination of the quality properties of beers. *Anal. Chim. Acta* **2006**, *571*, 167–174.
(29) Llario, R.; Inon, F. A.; Garrigues, S.; de la Guardia, M. Determination of quality parameters of beers by the use of attenuated total reflectance-Fourier transform infrared spectroscopy. *Talanta* **2006**, *69*, 469–480.
(30) Blanco, M.; Coello, J.; Iturriaga, H.; Maspoch, S.; Pages, J. NIR calibration in non-linear systems: different PLS approaches and artificial neural networks. *Chemom. Intell. Lab. Syst.* **2000**, *50*, 75–82.
(31) Han, Q. J.; Wu, H. L.; Cai, C. B.; Xu, L.; Yu, R. Q. An ensemble of Monte Carlo uninformative variable elimination for wavelength selection. *Anal. Chim. Acta*, in press.
(32) Macedo, M. G.; Laporte, M. F.; Lacroix, C. Quantification of exopolysaccharide, lactic acid, and lactose concentrations in culture broth by near-infrared spectroscopy. *J. Agric. Food Chem.* **2002**, *50* (7), 1774–1779.
(33) Ozaki, Y.; McClure, W. F.; Christy, A. A. *Near-Infrared Spectroscopy in Food Science and Technology*; John Wiley & Sons. Inc.: Hoboken, NJ, 2007.
(34) Williams, P. C., Sobering, D. C. How do we do it: a brief summary of the methods we use in developing near infrared calibrations. In *Near Infrared Spectroscopy: The Future Waves*; Davies, A. M. C., Williams, P. C., Eds.; NIR Publications: Chichester, U.K., 1996; pp 185−188.
(35) Wang, J. G. Analysis of composition and source of color, aroma, taste, type in rice wine. *China Brew.* **2004**, No. 4, 6−10.
(36) Yan, Y. L.; Zhao, L. L.; Han, D. H.; Yan, S.M. *Basic and Application of Near-Infrared Spectral Analysis*; China Light Industry Press: Beijing, 2005.
(37) Yu, H. Y.; Zhou, Y.; Fu, X. P.; Xie, L. J.; Ying, Y. B. Discrimination between Chinese rice wines of different geographical origins by NIRS and AAS. *Eur. Food Res. Technol.* **2007**, *225* (3−4), 313–320.
(38) Liu, L.; Cozzolino, D.; Cynkar, W. U.; Dambergs, R. G.; Janik, L.; O'neill, B. K.; Colby, C. B.; Gishen, M. Preliminary study on the application of visible-near infrared spectroscopy and chemometrics to classify Riesling wines from different countries. *Food Chem.* **2008**, *106* (2), 781–786.
(39) Cozzolino, D.; Smyth, H. E.; Gishen, M. Feasibility study on the use of visible and near-infrared spectroscopy together with chemometrics to discriminate between commercial white wines of different varietal origins. *J. Agric. Food Chem.* **2003**, *51*, 7703–7708.
(40) Lu, W. Z. *Modern Near Infrared Spectroscopy Analytical Technology*, 2nd ed.; China Petrochemical Press: Beijing, 2007.
(41) Buning-Pfaue, H. Analysis of water in food by near infrared spectroscopy. *Food Chem.* **2003**, *82*, 107–115.
(42) Osborne, B. G.; Fearn, T. *Near-Infrared Spectroscopy in Food Analysis*; Longman Scientific and Technical: New York, 1986.

Received for review March 30, 2008. Revised manuscript received June 16, 2008. Accepted June 20, 2008. We gratefully acknowledge the financial support provided by the National Key Technology R&D Program (Grant No. 2006BAD11A12) and the Program for New Century Excellent Talents in University (Grant No. NCET-04-0524).

JF800993E